INL/CON-16-39574
PREPRINT

Development of Electrical Capacitance Sensors for Accident Tolerant Fuel (ATF) Testing at the Transient Reactor Test (TREAT) Facility

Test, Research, and Training Reactors (TRTR)

Maolong Liu, Matthew Ryals, Amir Ali,
Edward Blandford, Colby Jensen,
Keith Condie, John Svoboda, Robert O'Brien

August 2016

Development of Electrical Capacitance Sensors for Accident Tolerant Fuel (ATF) Testing at the Transient Reactor Test (TREAT) Facility

Maolong Liu, Matthew Ryals, Amir Ali, Edward Blandford
Department of Nuclear Engineering, University of New Mexico

Colby Jensen, Keith Condie, John Svoboda and Robert O'Brien
Idaho National Laboratory

A variety of instruments are being developed and qualified to support the Accident Tolerant Fuels (ATF) program and future transient irradiations at the Transient Reactor Test (TREAT) facility at Idaho National Laboratory (INL). The University of New Mexico (UNM) is working with INL to develop capacitance-based void sensors for determining the timing of critical boiling phenomena in static capsule fuel testing and the volume-averaged void fraction in flow-boiling in-pile water loop fuel testing. The static capsule sensor developed at INL is a plate-type configuration, while UNM is utilizing a ring-type capacitance sensor. Each sensor design has been theoretically and experimentally investigated at INL and UNM. Experiments are being performed at INL in an autoclave to investigate the performance of these sensors under representative Pressurized Water Reactor (PWR) conditions in a static capsule. Experiments have been performed at UNM using air-water two-phase flow to determine the sensitivity and time response of the capacitance sensor under a flow boiling configuration. Initial measurements from the capacitance sensor have demonstrated the validity of the concept to enable real-time measurement of void fraction. The next steps include designing the cabling interface with the flow loop at UNM for Reactivity Initiated Accident (RIA) ATF testing at TREAT and further characterization of the measurement response for each sensor under varying conditions by experiments and modeling.

1. Introduction

The TREAT facility at INL was used historically to study fuel melting phenomenology, interactions between overheated fuel and coolant, and the transient fuel response of fuels for advanced reactor systems. With the recent decision to restart the TREAT facility, DOE Office of Nuclear Energy-sponsored ATF program is currently investigating a wide range of alternative fuel system technologies with the ultimate program mission to demonstrate fuel performance in a commercial power reactor by 2022 [1]. The ATF fuel irradiation program is broken up into four experimental testing series prior to commercial demonstration starting with drop-in capsule irradiation tests at the Advanced Test Reactor (ATR) at INL, PWR prototypical loop tests also at ATR, and transient testing at the TREAT facility under RIA and Loss of Coolant Accident events. To support experimental objectives and modeling and simulation data validation needs, a variety of instruments are being developed and qualified by INL to support the ATF and future transient irradiations at the TREAT facility [2].

For RIA events, the thermal hydraulic conditions experienced by fuel undergo a rapid transition from forced convection cooling to critical heat flux conditions. This rapid rise in heat flux in the fuel ultimately leads to film boiling conditions at the surface of the fuel clad resulting with high cladding temperatures and eventually the collapse of the surrounding vapor blanket. Though several experimental programs have been performed to measure fuel performance phenomena under RIA conditions, the time-dependent thermal hydraulic conditions at the fuel clad surface remain an area of high uncertainty [3] and thus a primary target for data collection intended for fuel performance model validation.

Performing accurate void fraction measurements in two-phase flow mixtures has historically been a challenge in the thermal-hydraulic community. A number of different techniques have been developed including the wire mesh method [4], X-ray scanning method [5, 6], Ultra-fast X-ray CT scanner, Gamma-ray attenuation method, Neutron radiography [7], Nuclear Magnetic Resonance (NRM) imaging [8], Bi-optical probe [9], Needle contact probes [10], Photography method, Conductance-type void fraction meter [11], Capacitance-type void fraction sensor, and ultrasonic method [4]. An exhaustive review of current void fraction measurement techniques can be found in Reference [12]. However, these methods either invasive (i.e. disturb the flow field) or are too complex or expensive for engineering application. Moreover, only some of these technologies are capable of real-time measurement under high-pressure and high-temperature conditions. A capacitance type sensor is a potentially attractive alternative due to the fact that it is a non-invasive measurement and can possibly meet the non-trivial functional I&C requirements imposed by RIA testing.

In this paper, we present ongoing research activities to develop a ring-type, two-phase flow capacitance-based void sensor for flowing water loop conditions and a plate-type void sensor for static capsule testing up to PWR pressure and temperature conditions. A capacitance sensor is a well-established technique for determining the concentration of components with different permittivity [13]. In 1967, Cimorelli and Evangelisti [14] developed a capacitance sensor to study bulk boiling at atmospheric pressure. Thereafter, various types of capacitance sensor were developed to measure flow regime, velocity vector flow fields [15] and void fraction, including flat-plate, concave, helical and multiple helical type. Abouelwafa and Kendall (1980) [16] designed six electrode types sensors to measure water-oil/water-air/oil-air two-phase flow void fraction. Shu et al. (1982) [17] performed static and dynamic calibration of their concave-type sensor for both stratified flow and vertical flow. For vertical flow, the sensor was first calibrated in a static test by inserting glass tubes into the center of the sensor and comparing with dynamic calibration tests using a quick-closing valve technique. For static calibration test, since the dielectric constant of glass is slightly bigger than that for air, a correction factor is proposed to account for the difference between glass and air [17]. In order to improve the stability and sensitivity, Huang, S. (1986) [18] designed a guard layer on the capacitance sensor to minimize the parasitic capacitance between the sensor and the environment. One disadvantage of the capacitance sensor is the non-uniformity of the distribution of sensitivity over the pipe cross-section and therefore differing responses to different flow regimes [13, 19]. As indicated by Strizzolo, C. N. and J. Converti (1993) [20] and Ceccio, S. and D. George (1996) [19], the response of concave-type sensors and ring-type sensors are strongly related to flow regime. For these sensors, the output capacitance is not proportional to the void fraction, and also depends on the flow regime. Therefore the calibration of the sensor is needed.

2. Principle of the capacitance-based void sensor

The measurement of capacitance of a conducting liquid, like water, is difficult because of equivalent resistance of the liquid [21]. Two methods can be utilized to cut-off the effect of the resistance (1) the sensor admittance has to be measured in high frequency range (≥ 80 MHz for water at 25.0 °C) [22], or (2) the sensor needs to be insulated from liquid. For the present study, the sensor has been insulated, as a results, the effect of the water resistance can be neglected. The effective capacitance of the sensor can be written as

$$C_e = \frac{C_\alpha C_s}{C_\alpha + C_s} \tag{1}$$

where the C_α is an idealized capacitance, which is proportional to the effective dielectric constant of water/steam or water/gas mixture. Table 1 shows relative dielectric constants of several materials used in the present study. Other parasitic capacitances including that to a grounded shield and to grounded elements are represented by C_s.

Table 1: Relative dielectric constant used in the present study

Material	**Phase**	**Relative dielectric constant**
Air (0 °C)	Gas	1.00054
Teflon	Solid	2.1
Polyvinyl chloride (PVC)	Solid	2.0 [23]
Pure water	Liquid	79.55 (25 °C) Depends on pressure and temperature at constant measurement frequency [24, 25]
Tap water	Liquid	78.5 (25 °C) [26]

The effective dielectric constant of two-phase flow can be further simplified following two models: (1) parallel model and (2) series model [27]. The corresponding effective dielectric constant for these two models are derived using a simplified electrical resistance approach. For the parallel model, it is assumed that a mixture of liquid and gas in the channel can be represented by two lumped capacitances in parallel, one containing gas as the dielectric, and the second filled with liquid [16] (see Figure 1). Therefore, the effective dielectric constant can be written as,

$$K_{ep} = \alpha K_g + (1-\alpha) K_l \tag{2}$$

In the case of the series model, the mixture can be modeled as two lumped capacitances in series, which results in the effective dielectric constant being written as,

$$\frac{1}{K_{es}} = \frac{\alpha}{K_g} + \frac{1-\alpha}{K_l} \tag{3}$$

where K_{ep} is the equivalent dielectric constant of two-phase mixture for parallel model, K_{es} is the equivalent dielectric constant of two-phase mixture for series model, α is the void fraction and K_l and K_g are the dielectric constant of water and gas, respectively.

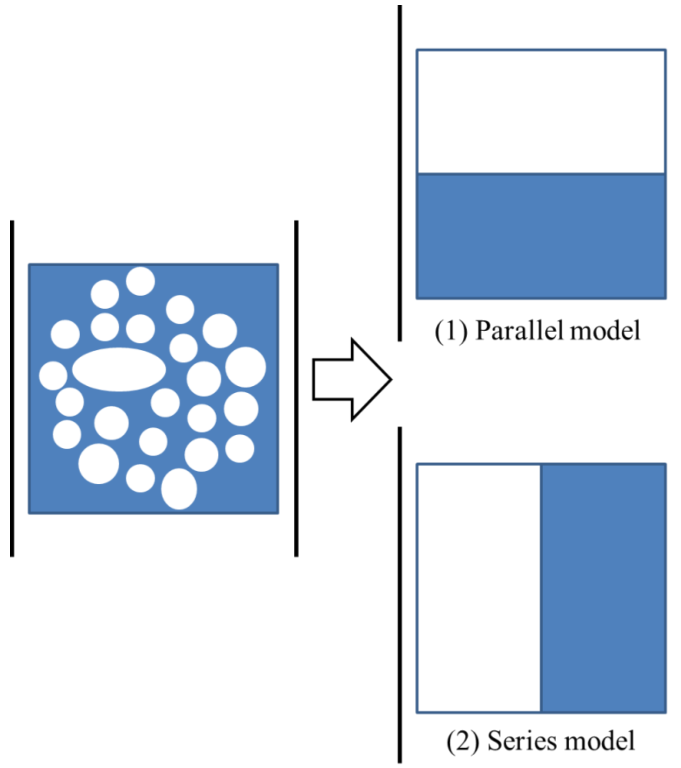

Figure 1 Effective dielectric constant models for two-phase flow

All two-phase mixtures fall between these two extreme cases [28]. The difference in effective dielectric constant between parallel and series distributions is estimated using equation (2) and (3) for water under PWR conditions (see Figure 2). There is little error in the bubbly flow (low void fraction) and droplet flow (high void fraction). However, it has over 50% error when the void fraction is around 0.5. The comparison of these two extreme cases shows the strong influence of the flow regime on the void sensor output. This error can be ignored only when the same flow regime is always obtained for each void fraction [20]. This analysis also provided guidance for the calibration work of the plate-type sensor and the ring-type sensor for vertical flow. Future calibration effect should mostly focus on these flow regimes that have relatively higher error.

3. Void sensor development at UNM for flow boiling conditions in loop tests

3.1 Sensor design

The main objective of the design was to build a ring-type void sensor that would be capable of measuring void fraction with low uncertainty. The ring-type void sensor, designed by UNM to measure the volume-averaged void fraction, is shown in Figure 3. The sensors consist of two identical rings as the sensing area and ground. The length of two rings is 0.5 times the tube inner diameter. A guard ring is placed outside of the sensors to minimize parasitic capacitance. The sensors and guard ring are shielded to minimize external interference. All connecting cables are SubMiniature version A (SMA) coaxial and relatively short in order to minimize internal parasitic capacitance and resistance.

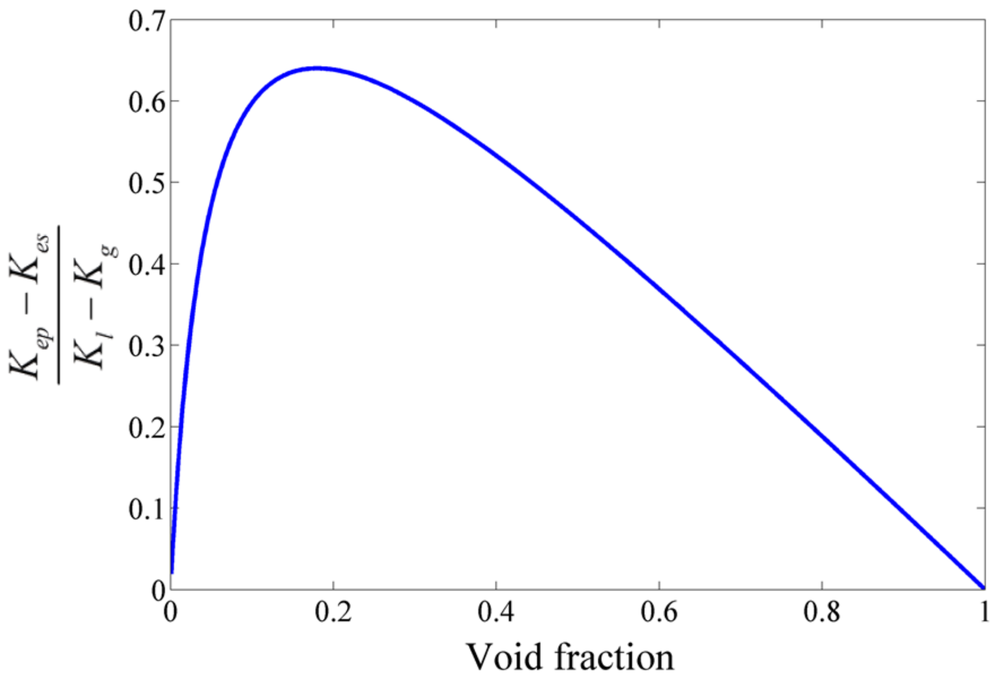

Figure 2 Difference in effective dielectric constant between parallel and series distributions

3.2. Measurement system

The circuit measuring the capacitance of the void fraction sensor should have low baseline drift, high and stable sensitivity, immunity to parasitic capacitances and immunity to external electrical interference [13]. The D100 Digital Capacitance Amplifier (D100) from MTI Instruments is utilized in the present study to measure the capacitance. A highly accurate buffer amplifier is utilized by the D100 to drive the sensor, guard and the coaxial cable shield at the same phase and amplitude as the sensing signal. This ensures that all parasitic capacitance effects are minimized, allowing the circuit to only respond to the capacitance present between the target surface and the sensing area (see Figure 3).

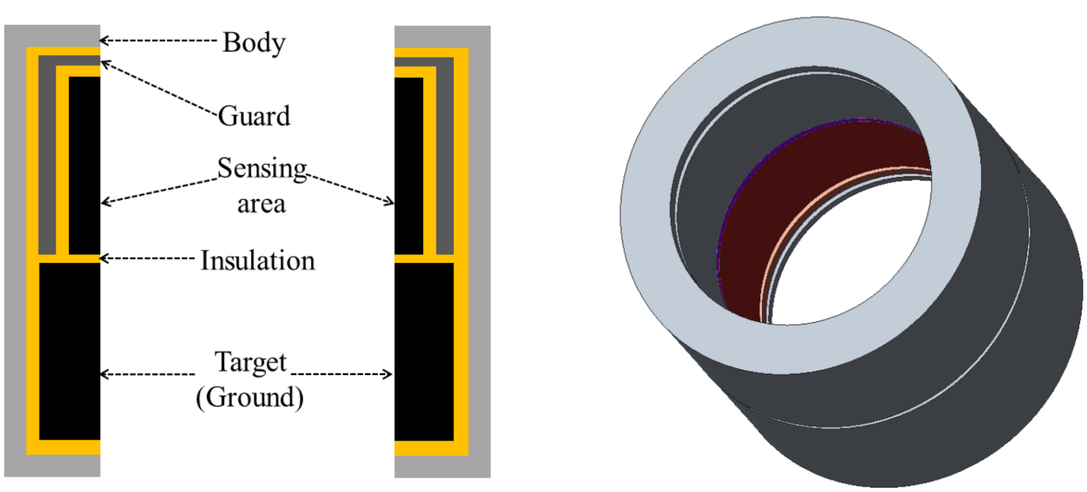

Figure 3 Schematic of void sensor designed by UNM

3.3 Calibration setup for stratified flow

The sensor was tested on a bench top with stratified flow so that liquid levels could be precisely controlled and measured. Since the fluid velocities do not affect the sensor reading, only static testing is carried out for this flow pattern to calibrate the sensor. As shown in Figure 4, the sensor is installed on a 24.0 inch long by 1.5 inch diameter PVC pipe. The stratified flow pattern was simulated simply by holding the sensor horizontally and by adding a measured volume of water.

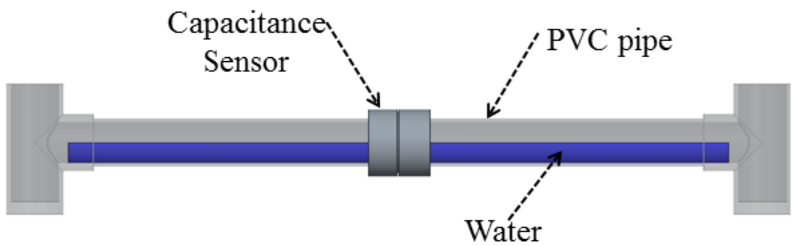

Figure 4 Calibration setup for stratified flow

3.4 Calibration results

Figure 5 shows the preliminary calibration results of normalized capacitance, C^*, as a function of void fraction for stratified flow. The normalized capacitance is defined as

$$C^* = \frac{C_\alpha - C_g}{C_w - C_g} \tag{4}$$

where C_w, C_g and C_α represent the capacitance for all water, all air, and measured values respectively. A number of calibration tests were performed by adjusting the depth of the water in the horizontal pipe to check the linearity of the capacitance-void-fraction relation. The experimental results show that the relation between the capacitance and void fraction is approximately linear when the void fraction is bigger than 0.15. Repeatability tests were also performed, and the results indicated that the variation in void fraction is less 2.0%. The theoretical value of the series model and the parallel model are also plotted in Figure 5. The calibration results are bounded by the theoretical curves.

4. Boiling sensor development at INL for static capsule testing

Application of a void sensor for in-pile measurement requires significant adaptation to address environment and facility constraints. Initial development efforts for the void sensor at INL have been focused on the sensor design and integration into the experimental device, instrument lead wire and data transmission design, and experiment environmental effects of water at PWR conditions (2250 psi and 280 ℃). The current sensor design is shown in Figure 6. The sensor is constrained to fit within a 1.5 inch inner diameter cylinder filled with water. The sensor will be immersed in the PWR water surrounding the test fuel specimen (0.374 inch outer diameter) in the center of the cavity. The sensor consists of two semi-circular-shaped plates that run the length of the test specimen, located between the plates. Metal sheathed single conductor coaxial cable will connect to the sensor plates within the high pressure capsule. The lead wire must pass out of the capsule through a feedthrough, extend the length of the core and beyond the reflector region of the TREAT reactor to a location above the rotating shield plug where it will pass through a buffer circuit to eliminate parasitic capacitance and other electromagnetic interferences between the buffer and the data acquisition system. Ongoing testing at INL is focused on understanding and optimizing sensor performance in water up to PWR conditions.

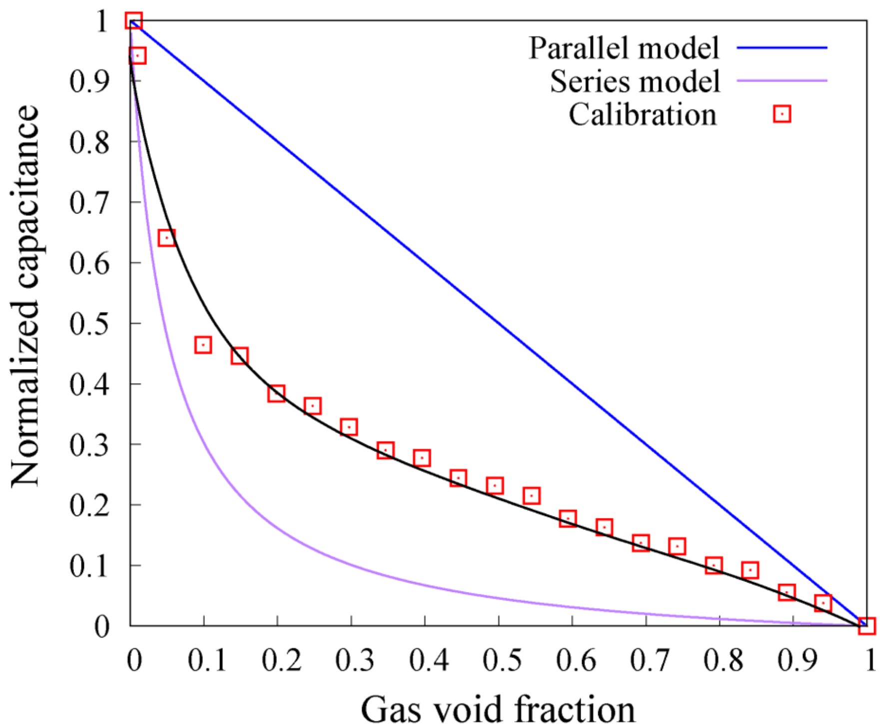

Figure 5 Calibration result for stratified flow

Simulations of the void sensor in the INL autoclave were performed using STAR-CCM+. Models were created to investigate current boiling detector design sensitivity to void presence and void location. A simplified, static two dimensional model of an axial cross section of the autoclave environment and the void sensor was created to represent capacitance with no void present, a layer of air around the simulated fuel rod, and air bubbles located at different locations between the sensors and fuel rod. The two cases with void had the same void volume. Figure 7 (a) shows an axial cross-section of the simulated geometry. A potential of +1V was placed on left terminal and -1V was placed on the right for all models, with no grounds present. The outer boundary of the autoclave was modeled as a zero flux condition. The material properties were taken at room temperature for these calculations.

Figure 7 (b)-(d) shows the calculated potential fields in the system for each of the three modeled cases. Table 2 provides the calculated capacitance corresponding to each case. A comparison of measured capacitance across the three models shows a deviation of ~7% from no void, to "nucleate" boiling. A comparison of the no void model to the "film boiling" model shows a drop of ~18% in measured capacitance. These preliminary results indicated that void near the surface of the rodlet will have greater effect on measured capacitance than void in the free volume. The results indicate promise of distinguishing film boiling from nucleate boiling phases.

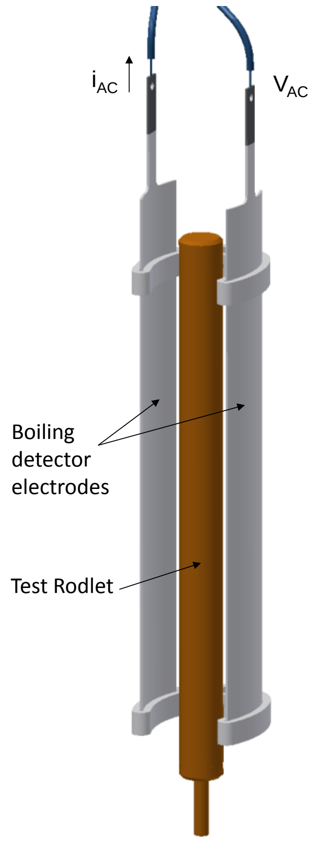

Figure 6 Void sensor design to be used in TREAT experiments in pressurized water capsules. The sensor will detect void created from rapid heating of the test specimen.

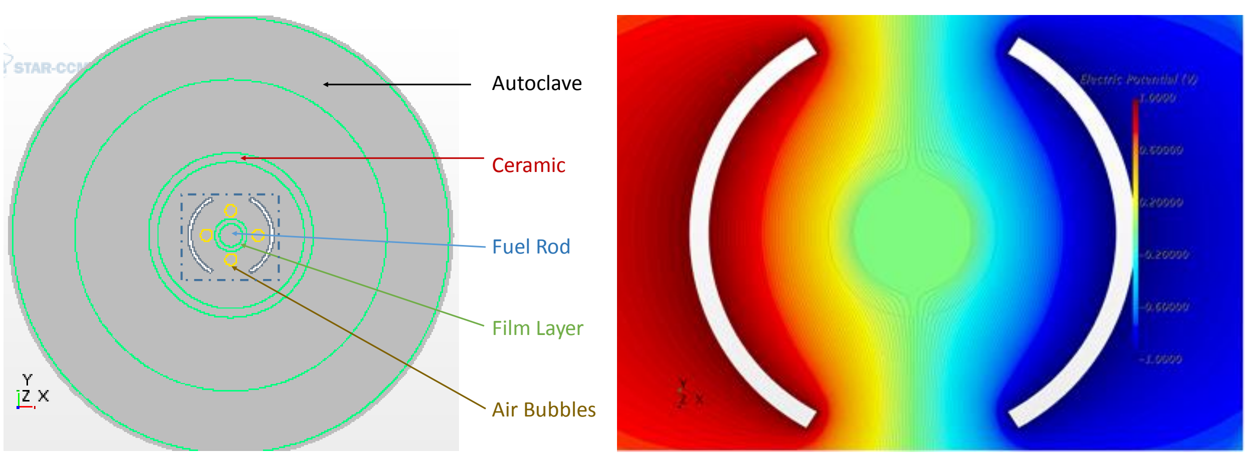

(a) (b)

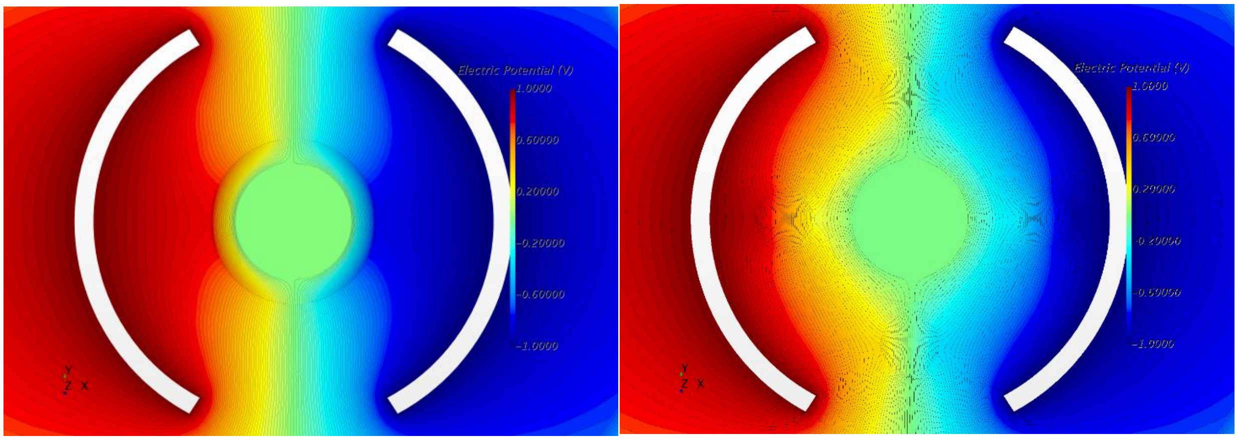

(c) (d)

Figure 7 (a) Axial cross-section of simulated environment. A zero flux condition was set on the autoclave wall, a +1V was set on the left terminal and -1V on the right terminal. Regions between parts represent water at 25 ℃; (b) Electric potential lines with no void present, calculated capacitance, C_m=2.02e-9 farads; (c) Electric potential lines in a system with 2.0 mm thick ring of air around fuel rod, C_M=1.65e-9 farads; (d) Electric potential lines in a system with 4 bubbles of equal area to film boiling study, C_M=1.87e-9 farads

Table 2 Calculated capacitance for 3 simulations

Model	**Calculated Capacitance (pF)**	**Percentage change in capacitance from no void model**
No void	2015.64	—
Film layer	1646.29	-18%
Nucleate boiling	1869.04	-7%

5. Conclusion

In this study, a custom designed void sensor and boiling detector were shown to provide the ability to detect bubbles in two-phase flow. The results indicate that the new sensor is capable for use in air/water two-phase flow measurements at low-temperature and low pressure conditions however additional work needs to be done to ensure the sensor can work in various flow regimes and flow boiling conditions. Initial calibration test of the void fraction sensor were carried out for stratified flow. The void fraction sensor is very sensitive to void fraction change for stratified flow. A parallel plate capacitive sensor design has been developed at INL for use in initial PWR transient testing in TREAT. The sensor has been shown to be sensitive to void detection up to 2250 psi and 280 ℃. The design has been developed specifically for in-core measurements requiring careful design and testing of instrument lead wire and signal filtering. Star-CCM+ has been shown to be a valuable tool to model the electrostatic field of the capacitive sensor to perform sensitivity studies. Simulations of the void sensor have been performed using STAR-CCM+ to show possibility to distinguish boiling regimes based on measured capacitance. Future work is focused on optimizing both sensors for void measurement in water up to PWR conditions. Continued modeling efforts will focus on the optimization of sensor design and placement to maximize sensitivity of measurements as well quantification of void fraction based on capacitance measurement.

Reference

1. Bragg-Sitton, S., *Development of Advanced Accident-Tolerant Fuels for Commercial LWRs.* Nuclear News, 2014. **March**: p. 83-91.
2. Woolstenhulme, N.E., et al. *TREAT Irradiation Vehicle Designs, Capabilities, and Future Plans*. in *PHYSOR 2016*. 2016. Sun Valley, Idaho, USA.
3. Beck, W., et al., *Nuclear Fuel Safety Criteria Technical Review*. 2 ed. 2012.
4. Fuangworawong, N. *Local void fraction measurement by using reflected ultrasonic intensity and wire mesh tomography in air-water bubbly flow*. 2007.
5. Hu, B., et al., *Development of an X-ray computed tomography (CT) system with sparse sources: application to three-phase pipe flow visualization.* Experiments in fluids, 2005. **39**(4): p. 667-678.
6. Kendoush, A.A. and Z.A. Sarkis, *Void fraction measurement by X-ray absorption.* Experimental thermal and fluid science, 2002. **25**(8): p. 615-621.
7. Buell, J., et al., *A neutron scatterometer for void-fraction measurement in heated rod-bundle channels under CANDU LOCA conditions.* International journal of multiphase flow, 2005. **31**(4): p. 452-472.
8. Majors, P.D., R. Givler, and E. Fukushima, *Velocity and concentration measurements in multiphase flows by NMR.* Journal of Magnetic Resonance (1969), 1989. **85**(2): p. 235-243.
9. Kiambi, S., et al., *Measurements of bubble characteristics: comparison between double optical probe and imaging.* The Canadian Journal of Chemical Engineering, 2003. **81**(3‐4): p. 764-770.
10. Fossa, M., *Design and performance of a conductance probe for measuring the liquid fraction in two-phase gas-liquid flows.* Flow Measurement and Instrumentation, 1998. **9**(2): p. 103-109.
11. Song, C.-H., M.K. Chung, and H.C. No, *Measurements of void fraction by an improved multi-channel conductance void meter.* Nuclear Engineering and Design, 1998. **184**(2): p. 269-285.
12. AESJ, *Advanced Measurement in Multiphase Flow*, ed. AESJ. 2003: Morikita Publishing Co., Ltd.
13. Xie, C., et al., *Design of capacitance electrodes for concentration measurement of two-phase flow.* Measurement Science and Technology, 1990. **1**(1): p. 65.
14. Cimorelli, L. and R. Evangelisti, *The application of the capacitance method for void fraction measurement in bulk boiling conditions.* International Journal of Heat and Mass Transfer, 1967. **10**(3): p. 277-288.
15. Reinecke, N. and D. Mewes, *Recent developments and industrial/research applications of capacitance tomography.* Measurement Science and Technology, 1996. **7**(3): p. 233.
16. Abouelwafa, M.S.A. and E.J.M. Kendall, *The use of capacitance sensors for phase percentage determination in multiphase pipelines.* Instrumentation and Measurement, IEEE Transactions on, 1980. **29**(1): p. 24-27.
17. Shu, M.T., C.B. Weinberger, and Y.H. Lee, *A simple capacitance sensor for void fraction measurement in two-phase flow.* Industrial & Engineering Chemistry Fundamentals, 1982. **21**(2): p. 175-181.
18. Huang, S., *Capacitance transducers for concentration measurement in multi-component flow processes*. 1986, University of Manchester, Institute of Science and Technology.
19. Ceccio, S. and D. George, *A review of electrical impedance techniques for the measurement of multiphase flows.* Journal of fluids engineering, 1996. **118**(2): p. 391-399.
20. Strizzolo, C.N. and J. Converti, *Capacitance sensors for measurement of phase volume fraction in two-phase pipelines.* Instrumentation and Measurement, IEEE Transactions on, 1993. **42**(3): p. 726-729.

21. Jaworek, A., A. Krupa, and M. Trela, *Capacitance sensor for void fraction measurement in water/steam flows.* Flow Measurement and Instrumentation, 2004. **15**(5): p. 317-324.
22. Jaworek, A. and A. Krupa, *Gas/liquid ratio measurements by rf resonance capacitance sensor.* Sensors and Actuators A: Physical, 2004. **113**(2): p. 133-139.
23. Davies, J., R. Miller, and W. Busse, *Dielectric properties of plasticized polyvinyl chloride.* Journal of the American Chemical Society, 1941. **63**(2): p. 361-369.
24. Uematsu, M. and E. Frank, *Static dielectric constant of water and steam.* Journal of Physical and Chemical Reference Data, 1980. **9**(4): p. 1291-1306.
25. Malmberg, C. and A. Maryott, *Dielectric constant of water from 0^o to 100 ^{o}C.* J Res Nat Bureau Stand, 1956. **56**: p. 1-8.
26. Canière, H., *Flow pattern mapping of horizontal evaporating refrigerant flow based on capacitive void fraction measurements*. 2009, Ghent University.
27. McKeen, T.R. and T.S. Pugsley, *The influence of permittivity models on phantom images obtained from electrical capacitance tomography.* Measurement Science and technology, 2002. **13**(12): p. 1822.
28. Beker, M., *Capacitive measurement technique for void fraction measurements in two phase pipe flow*. 2005, Delft University of Technology.